Quantum Chemical Study of the pK_a Control Mechanism for the Active Center in Bacteriorhodopsin and Its M Intermediate

Sawako Nakajima, Kazuki Ohno, Yoshio Inoue, and Minoru Sakurai*

Department of Biomolecular Engineering, Tokyo Institute of Technology,4259 Nagatsuta-cho, Midori-ku, Yokohama 226-8501, Japan

Received: December 11, 2002; In Final Form: January 22, 2003

In this study, integrated (MOZYME + DFT) method (Ohno et al. *Chem. Phys. Lett.* **2001**, *341*, 387.) is applied to elucidate how the pK_a's of retinal Schiff base (RSB) and Asp85 in bacteriorhodopisn (bR) are controlled by the surrounding protein matrix, especially a hydrogen bonding network involving RSB. The whole protein is divided into two layers. Layer 1 contains only the hydrogen bonding network and is treated at the DFT level of theory. The rest of the protein is calculated using a linear-scaling molecular orbital method called MOZYME that can explicitly take into account the protein three-dimensional structure. Here we focus our attention on the pK_a changes of RSB and Asp85 on going from the ground state to the M intermediate, because they are key factors of the proton translocation mechanism in bR. The three-dimensional structures of both states are taken from corresponding X-ray data. The calculation successfully reproduces the experimental fact that RSB and Asp85 form the zwitterions in the ground state. On the other hand, the fact that these residues are in the neutral form in the M intermediate is reproduced only when the side chain of Thr89 takes a special orientation capable of forming hydrogen bond(s) with Asp85. It is shown that such hydrogen bond formation and the disappearance of water 402 are the major factors stabilizing the neutral state of the (RSB + Asp85) system in the M intermediate. Finally, we discuss a role of Thr89 in the proton translocation process.

Introduction

Bacteriorhodopsin (bR) is a retinal protein that participates in the light-induced vectorial proton pumping in the purple membrane of *Halobacterium salinarum*.[1] The chromophore *all-trans*-retinal binds covalently to Lys216 via protonated Schiff base linkage. Light absorption triggers a sequential photoreaction cycle consisting of spectroscopically distinct intermediates J, K, L, M, N, and O.[2] During the photocycle, protein structural changes occur and cause proton translocation from the inside of the cell to the outside via Asp96, the Schiff base, Asp85, and Glu204 (or the Glu204-Glu194 region).[3−6]

It is thought that proton pumping originates in change of pK_a of the retinal Schiff base (RSB), and the vectoriality is controlled by pK_a's of ionizable groups and/or water molecules in the protein. The decrease in the pK_a of RSB and/or an increase in the pK_a of a neighboring group are the first steps that may induce the proton transfer. Therefore, the pK_a change of these groups, especially RSB, plays a crucial role in the proton-transfer activity of bR. One of the important steps in determining the unidirectionality of the proton transport is the L to M transition associated with proton transfer from RSB to Asp85. This process is part of the mechanism that causes the switch of the access of RSB from the extracellular side to the cytoplasmic side.[7,8]

In the chromophore binding pocket, several water molecules and some polar groups form a hydrogen bonding network, and a variety of experiments have indicated that during the photocycle this hydrogen bonding network is rearranged.[9−11] Several X-ray diffraction studies showed that in the M intermediate water 402 (W402) and water 406 (W406) become disordered and water 401 (W401) reorients so as to form a hydrogen bond with Asp212.[12−14] It is of great interest to investigate how the pK_a of RSB is controlled by the hydrogen bonding network.

It is known that the pK_a of the protonated RSB in methanol/water (1:1) solution is about 7.2,[15,16] while the pK_a in the bR ground state is shifted to above 12.4.[17,18] These facts indicate that the protein environment has a significant effect on the pK_a of RSB. Many computational studies have concerned the mechanism of such a pK_a control by the protein environment.

The density functional theory (DFT) level of calculation combined with a continuum solvent model has been applied to estimate the relative proton affinity of RSB to acetic acid as a model of Asp85.[19] The proton affinity of RSB is considerably smaller than that of acetic acid in vacuo. With an increase in dielectric constant of the surrounding continuum, the proton affinity of RSB becomes much closer to that of acetic acid. However, even when using a dielectric constant of $\epsilon = 4.0$, a value corresponding to the protein environment, the proton preferred to stay on the carboxyl group. Thus, the continuum calculation failed to reproduce the zwitterionic state of protonated RSB−aspartate in the bR ground state. It seems that the effect of heterogeneity of the protein environment, which is not taken into account in the implicit solvent model, is important to reproduce the relative proton affinity between RSB and its counterion Asp85. Other DFT studies have indicated that the existence of W402, located between RSB and Asp85, and the twisting of some double bonds near the Schiff base terminal are also responsible for stabilization of the protonation state of RSB.[20−22]

Recently, hybrid quantum mechanics/molecular mechanics (QM/MM) calculation including the whole protein revealed that, in the bR ground state, the zwitterionic state of protonated

* Corresponding author. E-mail: msakurai@bio.titech.ac.jp.

10.1021/jp027688h CCC: $25.00
Published on Web 03/05/2003

RSB−deprotonated Asp85 is 4.9 kcal mol^{-1} more stable than the neutral state, in which the proton is transferred from RSB to the carboxyl oxygen of the Asp85 side chain.[23] Alternatively, the pK_a values for bR have been evaluated by using a combined method of multisite titration with a model assuming macroscopic electrostatics with atomic detail (MEAD model).[24] Such a classical model showed that the calculated pK_a values for RSB and the ionizable groups which are on or near the ion transport chain were in reasonable agreement with the available experimental data. Most recently, we have developed an integrated (MOZYME + DFT) method for calculating the pK_a values of ionizable residues in a protein.[25] The whole protein was divided into two layers: the first layer involves a few residues in the active site and was treated at the DFT level of theory, and the rest of the system was described by a linear-scaling molecular orbital method called MOZYME. By integrating these different levels of theory according to the methodological framework of ONIOM, full quantum mechanical evaluation of the pK_a values became possible. Our previous study indicated that the calculated ΔpK_a value between the protonated RSB and Asp85 is dramatically improved by use of such an integration method compared with a conventional continuum model and a simple linear-scaling calculation. The above three studies clearly indicate that the pK_a values of the active site residues can be reasonably reproduced by using the theoretical methods that can explicitly take into account the high-resolution X-ray structural data.

Nowadays, in addition to the bR ground state, the X-ray structures of the M intermediate are available, which enables us to evaluate the pK_a values of the active site residues in the M intermediate and to understand why RSB is deprotonated to form protonated Asp85. In this study, we apply the integrated (MOZYME + DFT) method to both the ground state and the M intermediate. Our final goal is to understand how the pK_a of RSB is controlled by the hydrogen bonding network formed at the chromophore binding site and to identify amino acid residues that significantly contribute to the pK_a control. It will be shown that the orientation of the Thr89 side chain is a key factor causing the proton transfer from RSB to Asp85.

Methods

Here, we focused our attention on the following equilibrium in the active center of bR:

$$AH^+ + B^- \leftrightarrow A + BH$$

where AH^+, B^-, A, and BH are protonated RSB, deprotonated Asp85, deprotonated RSB, and protonated Asp85, respectively. The left- and right-hand sides in this reaction are the zwitterionic state of the (RSB + Asp85) system and its neutral state, respectively.

The pK_a values were evaluated according to the integrated (MOZYME + DFT) method recently developed by our laboratory.[25] In this method, the whole protein is divided into two layers. The first layer (layer 1) is treated at the DFT level of theory, and the rest of the system is described by the AM1 level of theory. According to this method, the total energy of the whole system is given by

$$E^{\mathrm{ONIOM}} = E^{\mathrm{MOZYME}}_{\mathrm{whole}} - E^{\mathrm{MOZYME}}_{\mathrm{layer1}} + E^{\mathrm{DFT}}_{\mathrm{layer1}} \quad (1)$$

where $E^{\mathrm{MOZYME}}_{\mathrm{whole}}$ is the energy of whole system calculated by the MOZYME method,[26] and $E^{\mathrm{DFT}}_{\mathrm{layer1}}$ and $E^{\mathrm{MOZYME}}_{\mathrm{layer1}}$ are the energies of layer 1 obtained from DFT and MOZYME calculations, respectively. E^{ONIOM} is obtained for each of the zwitterionic and neutral states. Then, by subtracting the former from the latter, the total energy difference is obtained as follows:

$$\Delta E^{\mathrm{ONIOM}} = \Delta E^{\mathrm{MOZYME}}_{\mathrm{whole}} - \Delta E^{\mathrm{MOZYME}}_{\mathrm{layer1}} + \Delta E^{\mathrm{DFT}}_{\mathrm{layer1}} \quad (2)$$

In general, the acid-dissociation constant pK_a of the acid HX at a given temperature T is given by

$$\mathrm{p}K_a = (G(H^+) + G(X^-) - G(HX)/2.303RT \quad (3)$$

where G represents the free energy of each species. In this study, we are concerned with the relative pK_a of AH^+ to BH in the above equilibrium reaction. The corresponding expression is given as follows:

$$\Delta \mathrm{p}K_a = -\Delta G/2.303RT \cong -\Delta E^{\mathrm{ONIOM}}/2.303RT \quad (4)$$

where ΔG is the free energy difference between the zwitterionic ($AH^+ + B^-$) state and the neutral (A + BH) state and it was approximated by $\Delta E^{\mathrm{ONIOM}}$ in eq 2.

The initial atomic coordinates of the bR ground state and the M intermediate were taken from the Protein Databank (PDB). For the bR ground state, we used the 1.55 Å structure of the wild-type bR reported by Luecke et al. (the PDB entry code is 1C3W).[27] For the M intermediate, the following four structures were used: the 1.88 Å structure of the E204Q mutant (the PDB entry code is 1F4Z),[13] the 2.00 Å structure of the wild-type M (the PDB entry code is 1KG8),[28] the 2.00 Å structure of the D96N mutant (the PDB entry code is 1C8S),[12] and the 2.50 Å structure of the wild type (the PDB entry code is 1DZE).[29] We added hydrogen atoms to these structures using the Insight II program.[30] The ionization states of the polar residues in the protein were assumed as follows: Arg82, Arg134, Asp212, and Glu194 were set to be ionized and Asp96, Asp115, and Glu204 to be protonated.[31,32] The positions of all the hydrogen atoms and the heavy atoms of all the side chains were optimized using the MOZYME method with the AM1 Hamiltonian.[33] Then, the conformation about the C6−C7 single bond was fixed to be planar trans. All the other geometries concerning the protein backbone were fixed to the experimental values. The geometry optimization was carried out separately for the zwitterionic ($AH^+ + B^-$) state and the neutral (A + BH) state. The energy of the whole system $E^{\mathrm{MOZYME}}_{\mathrm{whole}}$ in eq 1 was obtained for the corresponding optimized geometry. The geometry of the layer 1 system was also taken from the optimized geometry for the whole protein, except for the addition of link atoms to dangling bonds. $E^{\mathrm{MOZYME}}_{\mathrm{whole}}$ and $E^{\mathrm{MOZYME}}_{\mathrm{layer1}}$ were obtained by using the MOPAC2002 program[34] and $E^{\mathrm{DFT}}_{\mathrm{layer1}}$ were done by using the Gaussian 98 program.[35] All the DFT calculations were carried out at the level of B3LYP/6-31+G**.

Results

Selection of Layer 1. According to the X-ray structures of the bR ground state and the M intermediate, hydrogen bonding networks are formed in the chromophore binding pocket. As shown in Figure 1, these networks consist of RSB, Asp85, Asp212, Thr89, and Arg82 and several water molecules, which correspond to W401, W402, W406, and W407 in the bR ground state[27] and to W401, W405 and W407 in the M intermediate.[12] It is expected that the whole or a part of such a hydrogen bonding cluster system provides a significant contribution to the pK_a control of RSB. Thus, it should be treated at high level of theory and should be involved in layer 1 in eq 1.

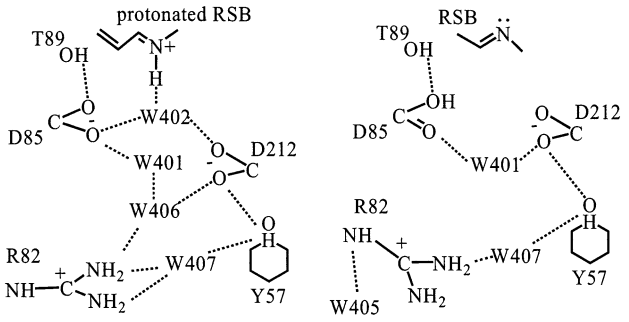

Figure 1. Schematic representation of the hydrogen bonding networks around the (RSB + Asp85) system in the bR ground state (left) and in the M intermediate (right). These illustrations were drawn by reference to Figure 4 of ref 12.

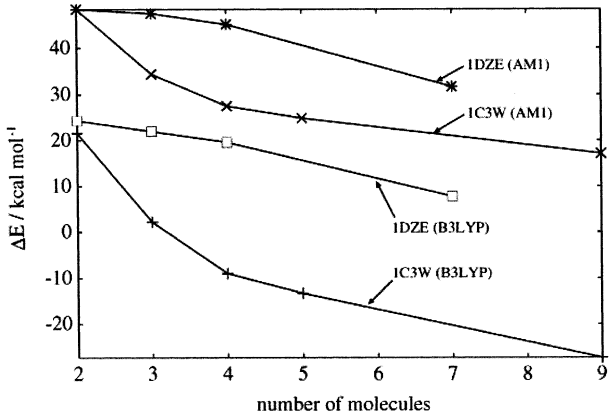

Figure 2. Dependence of ΔE_{layer1}^{AM1} and ΔE_{layer1}^{DFT} (eq 2) on the size of layer 1. The symbols × and + are the data for ΔE_{layer1}^{AM1} and ΔE_{layer1}^{DFT} obtained for the 1C3W structure, respectively. The symbols ∗ and □ are the data for ΔE_{layer1}^{AM1} and ΔE_{layer1}^{DFT} obtained for 1DZE structures, respectively. The abscissa represents the number of residues involved in layer 1. Those residues are listed in Table 2.

To determine the minimal size of layer 1, we examined the dependence of $\Delta E_{layer1}^{MOZYME}$ and ΔE_{layer1}^{DFT} on the number of residues picked up from the above hydrogen bonding network. Figure 2 shows the results for the bR ground state and the M intermediate, and Table 1 lists the residues involved in each cluster system that corresponds to each point on the abscissa of Figure 2. With an increase in the number of residues, $\Delta E_{layer1}^{MOZYME}$ and ΔE_{layer1}^{DFT} for the same protein structure tend to change in a fashion nearly parallel to each other. To interpret this result, eq 2 is rewritten as follows:

$$\Delta E^{ONIOM} = \Delta E_{whole}^{MOZYME} - (\Delta E_{layer1}^{MOZYME} - \Delta E_{layer1}^{DFT})$$

Figure 2 indicates that the second term on the right-hand side of this equation becomes constant with an increase in the size of layer 1. This means that the ΔE^{ONIOM} value becomes independent of the size of layer 1 if a sufficient number of the active site residues including RSB are involved in layer 1. According to Figure 2, a cluster system having more than five molecules, including RSB, is required to satisfy this condition. Finally, layer 1 was selected as follows: layer 1 for the bR ground state contains of nine molecules and that for the M intermediate contains seven molecules. Those molecules involved in layer 1 are listed in Table 1. Unless otherwise noted, layer 1 described below corresponds to any of them.

Relative pK_a Value of RSB to Asp85 in the bR Ground State. In the bR ground state, the experimental pK_a value of protonated RSB is >12.4 and that of Asp85 is about 2.[36] In a high pH region, the alkaline denaturation of bR starts to occur and the value of 12.4 seems to be a lower limit for the pK_a of RSB. Thus, the experimental ΔpK_a value in the bR ground state should be >10.4, which means that the zwitterionic state is considerably more stable compared to the neutral state. The calculated ΔpK_a value (eq 4) based on the 1C3W structure is summarized in Table 2, where the contribution of each energy term on the right-hand side of eq 2 is listed. For this X-ray structure, the value of $\Delta E_{whole}^{MOZYME}$ was 5.4 kcal mol^{-1}, which indicates that the pK_a of Asp85 was higher than that of the protonated RSB by 3.9 pK_a units. Thus, the pure semiempirical calculation for the whole protein failed to reproduce the experimental result, even for the direction of the pK_a shift. However, the calculated ΔpK_a value was dramatically improved by use of the ONIOM method. Then, ΔE^{ONIOM} has a value of −39.0 kcal mol^{-1}, corresponding to a ΔpK_a value of 28.5. Such a large negative value of ΔE^{ONIOM} (or a large positive ΔpK_a value) arises from the fact that the value of ΔE_{layer1}^{DFT} was much smaller than that of $\Delta E_{layer1}^{MOZYME}$. As described in the previous study,[25] this means that the energy of a π-conjugated system such as RSB is improved by use of DFT. Therefore, it can be said that the integrated (MOZYME + DFT) method successfully reproduced the ΔpK_a value in the bR ground state.

The contribution of ΔE_{layer1}^{DFT} to the total ONIOM energy ΔE^{ONIOM} (−39.0 kcal mol^{-1}) was −27.4 kcal mol^{-1}. This term is a major factor stabilizing the zwitterionic state of the (RSB + Asp85) system. On the other hand, the difference between ΔE_{layer1}^{DFT} and ΔE^{ONIOM} corresponds to the contribution of the rest of the protein, where electronic polarization and side chain reorientation are induced in response to the proton transfer in layer 1. This contribution was −11.6 kcal mol^{-1} (= −39.0 − (−27.4)), and thus the protein environment also significantly contributes to the increase of the ΔpK_a values.

From Table 1, we can know which residues in layer 1 contribute to stabilization of the zwitterionic state in the bR ground state. The third and fourth columns in this table indicate how the values of ΔE_{layer1}^{DFT} and ΔpK_a change with an increase in the size of the cluster system mentioned above. By adding W402 to the minimal system (RSB + Asp85), the ΔpK_a value increases by 14.1 (= −1.7 − (−15.8)). Next, by adding Thr89 to this three-molecule cluster, the ΔpK_a value increases by 8.3 (=6.6 − (−1.7)). Furthermore, by adding W401 to the four-molecule cluster, the ΔpK_a value increases by 3.1 (=9.7−6.6). The net contribution of the other residues in layer 1 is 10.3 (=20.0 − 9.7). These results show that the main contributors are W402, Thr89, and W401, and the sum of their contributions is 25.5 pK_a units (=14.1 + 8.3 + 3.1). The result that W402 and Thr89 significantly affect the ΔpK_a is consistent with that from the previous QM/MM study.[23]

Relative pK_a Value of RSB to Asp85 in the M Intermediate. Table 2 also shows the relative pK_a value of RSB to Asp85 for each X-ray structure of the M intermediate. In the M intermediate, the experimental pK_a value of RSB is 8.2−8.3,[37] which was determined for the D96N mutant, and that of Asp 85 is >11.[38] Thus, the experimental ΔpK_a value in the M intermediate should be < −2.8. Only when the initial structure was taken from 1DZE, the calculated ΔpK_a exhibited a negative value of −6.8, consistent with the experimental data. For the other X-ray structures (1F4Z, 1KG8, and 1C8S), the calculation indicated that the neutral state was less stable than the zwitterionic state.

From comparison of the energy terms on the right-hand side of eq 2 (see Table 2), there were found two factors responsible for such a larger lowering of ΔpK_a in the 1DZE structure, in

TABLE 1: Dependence of E_{layer1}^{DFT} and ΔpK_a on the Number of Residues Involved in Layer 1

no. of residues[c]	bR[a] residues included	bR[a] ΔE_{layer1}^{DFT}[d]	bR[a] ΔpK_a[e]	M[b] residues included	M[b] ΔE_{layer1}^{DFT}[d]	M[b] ΔpK_a
2	RSB, D85	21.6	−15.8	RSB, D85	24.3	−17.7
3	RSB, D85, W402	2.3	−1.7	RSB, D85, T89	22.0	−16.1
4	RSB, D85, W402, T89	−9.0	6.6	RSB, D85, T89, W401	19.6	−14.3
5	RSB, D85, W402, T89, W401	−13.3	9.7			
7[f]				RSB, D85, W401, T89, W407, D212, R82	7.8	−5.7
9[g]	RSB, D85, W402, T89, W401, D212, R82, W406, W407	−27.4	20.0			

[a] Calculated for 1C3W of the bR ground state. [b] Calculated for 1DZE of the M intermediate. [c] Corresponding to the abscissa of Figure 2. [d] The energy is given in kcal mol^{-1}. [e] This ΔpK_a value was obtained by use of the following equation: $\Delta pK_a \cong -\Delta E_{layer1}^{DFT}/2.303RT$. Thus, it involves only the contribution of layer 1. [f] Layer 1 for the M intermediate. [g] Layer 1 for the bR ground state.

TABLE 2: Values of ΔE^{ONIOM}, Its Components, and ΔpK_a Obtained for Different X-ray Structures of the bR Ground State and the M Intermediate

	bR 1C3W	M 1F4Z	M 1KG8	M 1C8S	M 1DZE
$\Delta E_{whole}^{MOZYME}$[a]	5.4	−37.7	19.3	22.7	33.1
$\Delta E_{layer1}^{MOZYME}$[a]	17.0	16.3	27.5	27.7	31.6
ΔE_{layer1}^{DFT}[a]	−27.4	−11.3	−2.0	2.3	7.8
ΔE^{ONIOM}[a]	−39.0	−65.3	−10.2	−2.7	9.3
ΔpK_a[b]	28.5	47.7	7.4	2.0	−6.8

[a] Energy terms appearing in eq 2. They are given in kcal mol^{-1}. [b] The pK_a difference calculated from ΔE^{ONIOM} by use of eq 4. This corresponds to the value obtained by subtracting the pK_a of Asp85 from that of RSB.

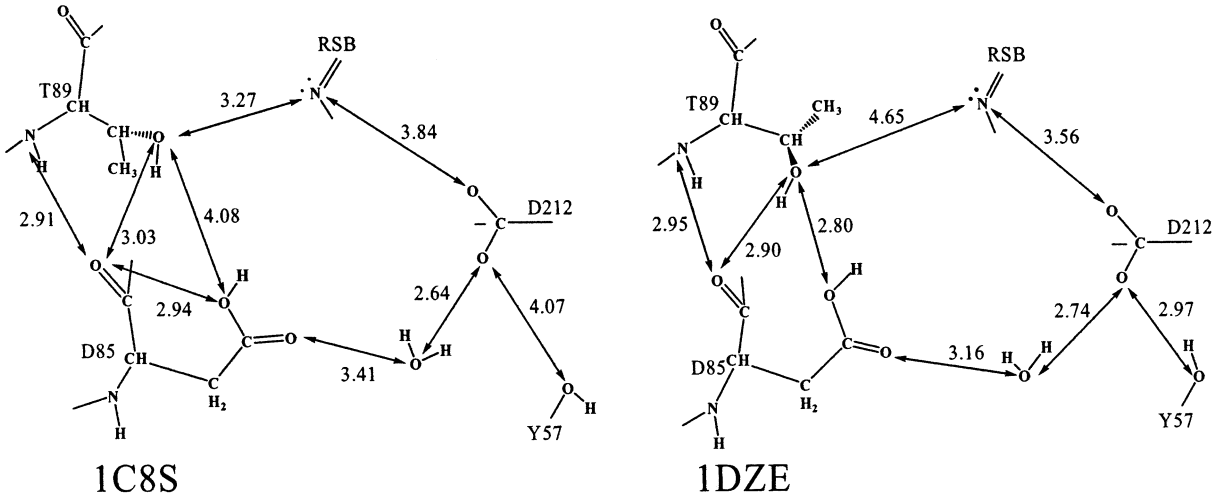

Figure 3. Examples of optimized structures of the retinal binding site in the M intermediate. The structure from 1C8S has model A orientation for the side chain of Thr89 (left), and that from 1DZE has model B orientation. The detailed explanation of models A and B is given in Figure 4.

other words, a larger increase in ΔE^{ONIOM}. First, the value of ΔE_{layer1}^{DFT} for the 1DZE structure was larger than those for the other structures. Second, the difference ($\Delta E^{ONIOM} - \Delta E_{layer1}^{DFT}$) had a positive value of 1.5 kcal mol^{-1} for the 1DZE structure, but those for the other structures had negative values. This means that, only in the case of 1DZE, the protein environment surrounding layer 1 contributes to the decrease of the ΔpK_a values, although its contribution (1.5 kcal mol^{-1}) is smaller in magnitude than that in the case of the bR ground state (|−11.6|).

To explore the reason the 1DZE structure provided the larger ΔE_{layer1}^{DFT} value, we compared the geometric parameters of layer 1 between 1DZE and the other structures, including the bR ground state structure. There were found significant differences in several interatomic distances characterizing the hydrogen bonding network of layer 1. Particularly, large differences were found for the distances between the side chain oxygen of Thr89 and the Schiff base nitrogen and between this oxygen and the carboxyl oxygen of Asp85. For example, as illustrated in Figure 3, the former and latter distances in 1DZE are 4.7 and 2.8 Å, respectively, while those in 1C8S are 3.3 and 4.1 Å. Furthermore, from comparison of the side chain conformations of the amino acid residues in layer 1, two types of conformational states were found for the side chain of Thr89 and they were denoted as model A and model B (see Figure 4). For example, the Thr89 side chains of 1C8S and 1DZE had the model A and B conformations, respectively (see Figure 3). In model A, the OH group of Thr89 is directed to the Schiff base nitrogen, while in model B, it is directed to the carboxyl oxygen of Asp85. Table 3 summarizes the data for the dihedral angle ϕ, defined in Figure 4, before and after the geometry optimization. Only for 1DZE is the optimized dihedral angle a large positive value of 163.2°, corresponding to model B, while for the other structures, the optimized values of ϕ are around −65.4°, corresponding to model A. Thr89 in the bR ground state also had the model A conformation.

Role of Thr89 in pK_a Control. To evaluate the effect of the side chain orientation of Thr89 on pK_a control, we manually rotated the dihedral angle ϕ of the side chain of Thr89 from

TABLE 3: Dihedral Angle ϕ of the Side Chain of Thr89 before and after Geometry Optimization in the bR Ground State and the M Intermediate

	bR	M			
	1C3W A	1F4Z A	1KG8 A	1C8S A	1DZE B
initial ϕ angle[a]	−70.7	−63.4	−64.5	−65.4	134.9
optimized ϕ angle[a]	−58.0	−64.5	−70.6	−65.3	163.2

[a] The definition of the angle ϕ is given in Figure 4. Angles are given in degrees.

TABLE 4: Dependence of ΔE^{ONIOM} and ΔpK_a on the Side Chain Orientation of Thr89

	bR		M							
	1C3W		1F4Z		1KG8		1C8S		1DZE	
	A[a]	B[a]	A	B	A	B	A	B	A	B
ΔE^{ONIOM} [b]	−39.0	−13.7	−65.3	−25.4	−10.2	−6.0	−2.7	16.7	−29.4	9.3
ΔpK_a[c]	28.5	10.0	47.7	18.5	7.4	4.4	2.0	−12.2	21.5	−6.8

[a] A and B are the models A and B shown in Figure 4. [b] The energy is obtained from eq 2 and given in kcal mol^{-1}. [c] Obtained from eq 4.

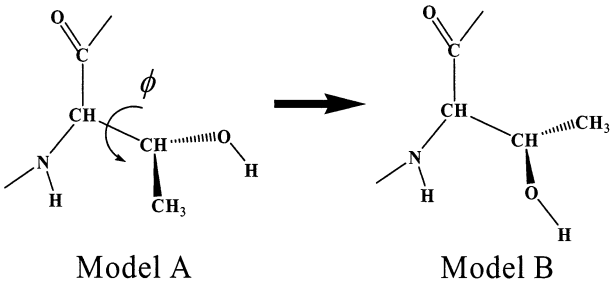

Figure 4. Two different orientations of the side chain of Thr89 found in the X-ray structures of the M intermediate and the definition of the dihedral angle ϕ. The two orientations are denoted as models A and B. The dihedral angle ϕ is defined as the rotation angle about the $-C_\alpha-C_\beta-$ bond and is zero when the side chain oxygen takes cis conformation with respect to the backbone carbonyl carbon (C*). The ϕ values of models A and B are in ranges of −70° to −60° and 130° to 160°, respectively.

the original X-ray values which are given in Table 3. For 1C3W, 1F4Z, 1KG8, and 1C8S, the angle ϕ was set to 134.9° by a rotation of 200°, leading to the model B conformation. For 1DZE, the angle ϕ was set to −65.4° by a rotation of 160°, leading to the model A conformation. Starting from these modified structures, the geometry optimization for the whole protein was carried out again.

Table 4 shows the relative ONIOM energy ΔE^{ONIOM} and the resultant ΔpK_a values for the two conformational states of Thr89 (model A and model B) for each X-ray structure. Irrespective of the X-ray structures used, the ΔpK_a values were always lowered on going from model A to B. This indicates that the side chain orientation of Thr89 is a common factor regulating ΔpK_a. Interestingly, in the case of 1DZE, the inverse transformation from model B (real structure) to model A leads to an unfavorable result with a positive ΔpK_a value. Therefore, the side chain orientation of Thr89 may act as a switch that regulates the ionization state of the (RSB + Asp85) system.

As expected, it was found that the rotation of the side chain of Thr89 caused the rearrangement of the hydrogen bond network around the (RSB + Asp85) system. Table 5 shows the interatomic distances measured from the side chain oxygen of Thr89 to the Schiff base nitrogen (T89O−SBN), to the side chain oxygen of Asp85 (T89O−D85O), or to the backbone carbonyl oxygen of Asp85 (T89O−D85O*). On going from model A to B, the distance T89O−SBN increased, while except for 1C3W the distance T89O−D85O tends to decrease. In the zwitterionic state with the model A conformation, the distances of T89O−SBN are relatively short (3.1−3.4 Å), and thus there should be electrostatic attraction (or hydrogen bond) between the side chain oxygen of Thr89 and the proton on the Schiff base nitrogen. However, in model B, such an interaction disappears due to the increase in the distance of T89O−SBN (4.3−4.6 Å). Therefore, irrespective of the X-ray structures used, the stability of the zwitterionic state should be decreased on going from model A to model B, which clearly accounts for the common tendency found in ΔE^{ONIOM} (Table 4). The 1DZE structure in the neutral state has remarkably small values for the distances T89O−D85O and T89O−D85O* when it takes the original model B conformation: the values of them are 2.8 and 2.9 Å, respectively. This means that the side chain oxygen of Thr89 forms stronger hydrogen bonds with Asp85, probably contributing to the stabilization of the neutral state, that is, a small ΔpK_a value of −6.8 (Table 4).

Table 6 summarizes the ONIOM energies (ΔE^{ONIOM} in eq 1) for all the structural models studied here. Among the 1C3W-based four models, the energy becomes lowest in the zwitterionic state with the model A conformation, consistent with the actual ground state structure. Similarly, among the 1DZE-based four models, the energy becomes lowest in the neutral state with the model B conformation, again consistent with the actual M intermediate structure. Therefore, the 1C3W and 1DZE structures not only provide the correct prediction for the ΔpK_a values but also are energetically reasonable.

Discussion

The integrated (MOZYME + DFT) calculation successfully reproduced the experimental fact that in the bR ground state the pK_a of RSB is larger than that of Asp85 by >10 units, and thereby the zwitterionic state of the (RSB + Asp85) system is more stable than the neutral state. As described in Table 2, a major factor causing the stabilization of the zwitterionic state is W402, which is located between RSB and Asp85. According to the X-ray studies, this water molecule disappears in the M intermediate.[12−14] On the other hand, an early ab intio molecular orbital study on the proton transfer between a Schiff base model and a carboxylate group[39] indicated that in vacuo the carboxylate attracts the proton and the neutral state is preferentially formed. Thus, when we started this work, it was expected that the occurrence of the neutral state in the M intermediate was easily reproduced by the calculation. However, we encountered unexpected results when the three-dimensional structure of the protein was explicitly taken into account in the calculation. As shown in Table 2, our integrated (MOZYME + DFT) method gave positive values for the ΔpK_a based on the three X-ray

TABLE 5: Distance (Å) between Thr89 and the (RSB + Asp85) System in Various Structural Models Studied

	model A			model B		
	T89O−SBN[a]	T89O−D85O[b]	T89O−D85O* [c]	T89O−SBN[a]	T89O−D85O[b]	T89O−D85O* [c]
			Zwitterionic State[d]			
1C3W	3.4	2.8	3.4	4.3	4.0	4.9
1C8S	3.1	3.7	3.1	4.6	3.6	3.8
1DZE	3.3	3.6	2.8	4.6	3.1	3.0
			Neutral State[e]			
1C3W	3.5	3.0	3.2	4.4	3.9	4.8
1C8S	3.3	4.1	3.0	4.6	3.6	3.7
1DZE	3.5	4.2	2.9	4.7	2.8	2.9

[a] Distance between the side chain oxygen of Thr89 and the Schiff base nitrogen. [b] Distance between the side chain oxygen of Thr89 and the side chain oxygen of Asp85. [c] Distance between the side chain oxygen of Thr89 and the backbone oxygen of Asp85. [d] The zwitterionic state of the (RSB + Asp85) system. [e] The neutral state of the (RSB + Asp85) system.

TABLE 6: ONIOM Energies (E^{ONIOM} in eq 1, Given in kcal mol^{-1}) for Various Structural Models of the bR Ground State and the M Intermediate

		M			
	bR 1C3W	1F4Z	1KG8	1C8S	1DZE
			Zwitterionic State[a]		
model A	−8 876 084.7	−8 810 079.3	−8 488 909.6	−7 816 826.6	−8 853 323.2
model B	−8 876 045.4	−8 810 060.3	−8 488 901.6	−7 816 822.2	−8 853 317.5
			Neutral State[b]		
model A	−8 876 045.8	−8 810 014.1	−8 488 899.5	−7 816 823.9	−8 853 293.8
model B	−8 876 031.7	−8 810 034.9	−8 488 895.6	−7 816 838.9	−8 853 326.8

[a] The zwitterionic state of the (RSB + Asp85) system. [b] The neutral state of the (RSB + Asp85) system.

structures (1F4Z, 1KG8, and 1C8S) which we first adopted as initial structures of the M intermediate. We could not reproduce the correct ΔpK_a value of the M intermediate until the 1DZE structure was adopted. From detailed comparison of these X-ray structures, it was found that the 1DZE structure has unique orientation in the side chain hydroxyl group of Thr89. As a result, the side chain of Thr89 can form strong hydrogen bonds with the side chain of Asp85, leading to the stabilization of the neutral state and to the decrease in the ΔpK_a (Tables 3−5). The most recent X-ray structure (PDB entry code: 1M0M) of the M intermediate,[40] which was published after the finish of the present study, also indicates the occurrence of such a hydrogen bond: the distance between the side chain oxygen of Thr89 and that of Asp85 is 2.7 Å.

Recent polarized FTIR studies have provided the rigorous evidence that there exists a hydrogen bond between Thr89 and Asp85 under near-physiological conditions.[41,42] Those studies revealed that the OH group of Thr89 forms a strong hydrogen bond with one of the side chain oxygen atoms of Asp85 in the bR ground state and this hydrogen bond is further strengthened through the M intermediate, where the hydrogen acceptor is the C−O−H group of protonated Asp85. To compare these FTIR results with our calculated ones, we again examine the geometries of the hydrogen bonding network around RSB. In the M intermediate based on the original 1DZE structure, the side chain OHs of Thr89 and Asp85 are connected through two hydrogen bonds: one is between the side chain OH of Thr89 and the carboxyl group of Asp85 and the other is between the side chain OH of Thr89 and the main chain carbonyl group of Asp85 (see the data for the neutral state of 1DZE in Table 5). On the other hand, in the bR ground state based on the 1C3W structure, these residues are connected through only one hydrogen bond formed between the side chain OH of Thr89 and the carboxyl group of Asp85 (see the data for the zwitterionic state of 1C3W). As a result, the number of hydrogen bonds in which Thr89 participates is larger in the M intermediate than in the bR ground state, which is qualitatively consistent with the above FTIR results.

Thr89, which is located one turn above Asp85 on the C-helix, is in a good position to interact with both RSB and Asp85 and hence to control the proton translocation between them. A variety of studies have provided important information that Thr89 plays a certain role in proton transfer from L to M. For example, a mutation study showed that the T89N substitution affects primarily the L to M transition, slowing it approximately 3−5-fold relative to the wild-type bR, but the kinetics of the M to N transition are almost identical to the wild type.[43] Thus, it is of great interest to investigate the possibility of the proton translocation pathway through Thr89. We attempted to derive three hypothetical states from the 1DZE structure. For example, with keeping the geometry of 1DZE, only the carboxyl proton of Asp 85 is transferred so as to protonate the Schiff base nitrogen, and subsequently the geometry optimization for all the hydrogen and side chain heavy atoms was performed. The resulting zwitterionic state is shown in Figure 5b. In a similar way, we obtained the other two states: Figure 5a is different in both the protonation state of RSB and the side chain orientation of Thr89 from the original 1DZE structure, and Figure 5c is different only in the latter factor from the original one. In view of these structures, we can assume the following hypothetical proton pathway. Structure a corresponds to a state before the proton transfer, where the hydroxyl oxygen of the Thr89 side chain is located with keeping nearly equal distances from both the Schiff base nitrogen and the carboxyl oxygen of Asp85. Thus, in this state, the double proton transfer may be possible from the Schiff base proton to the hydroxyl oxygen of Thr89 and from the hydroxyl proton of Thr89 to the carboxyl oxygen of Asp85. As a result, structure c is formed but at this stage the orientation of the Thr89 side chain is still in model A. Finally, its orientation changes to model B to yield structure d, corresponding to the M intermediate. As a whole, structure c is

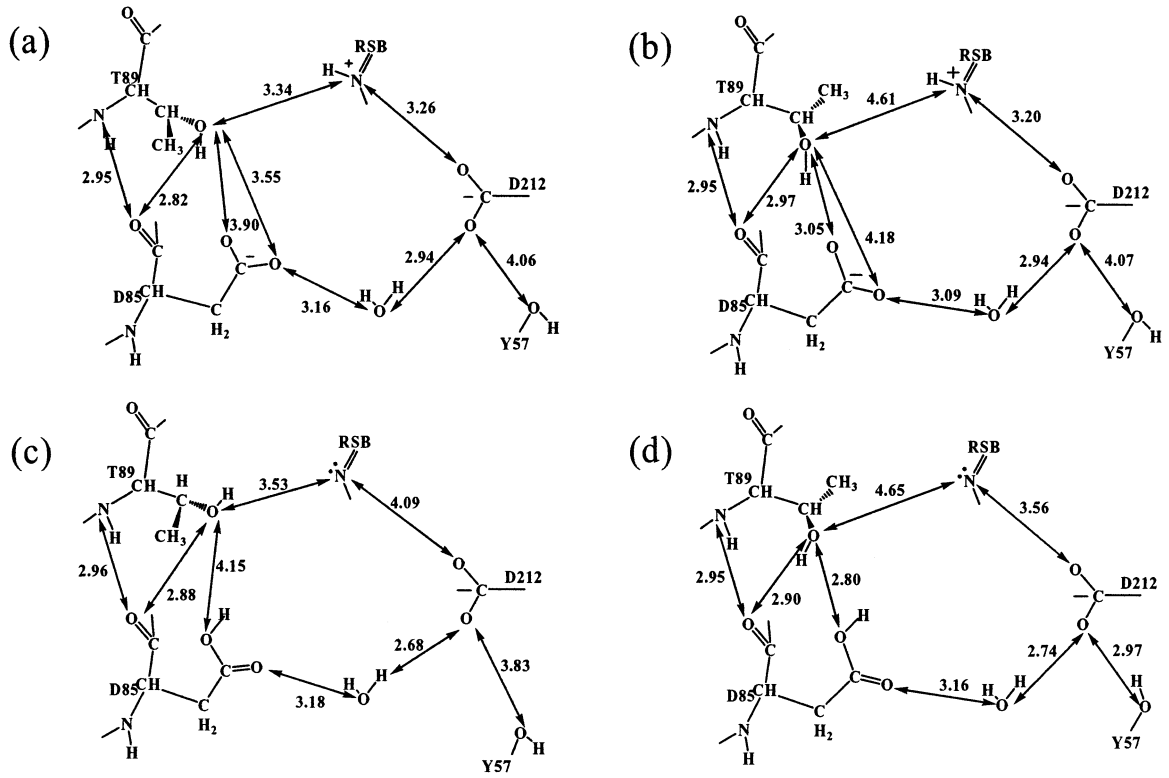

Figure 5. Three hypothetical states (a)−(c) derived from the 1DZE structure and the 1DZE itself (d). (a) and (b) correspond to the zwitterionic state of the (RSB + Asp85) system and (c) and (d) to the neutral state. (a) and (c) both have model A orientation for the Thr89 side chain, and (b) and (d) both have model B orientation.

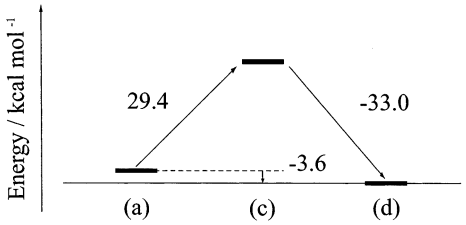

Figure 6. Relative energies among structures (a), (c), and (d) and a hypothetical proton-transfer pathway mediated by Thr89.

an intermediate state (or near transition state) for the proton transfer considered here.

The total energies for structures a−d are given in Table 6, and Figure 6 shows the relative energies among (a), (c) and (d). The energy difference between (a) and (c) and between (c) and (d) is 29.4 and 33.0 kcal mol^{-1}, respectively. Thus, there are large energy barriers for both the forward reaction from (a) to (d) and the back reaction from (d) to (a). The forward reaction of Figure 6 does not necessarily correspond to the real pathway from the L to M intermediates, because (a) is the hypothetical state derived from the 1DZE structure. However, the back reaction seems to involve any information about a role of Thr89, because structure d corresponds to the real M intermediate based on 1DZE. It can be inferred from this energy diagram that the back proton transfer from the M intermediate is blocked due to a high reaction barrier generated by rotation of the Thr89 side chain. Consequently, Thr89 may be responsible for the occurrence of unidirectional proton transfer in bR.

Conclusion

The integrated (MOZYME + DFT) calculation successfully reproduced the relative pK_a values of RSB to Asp85 in both the bR ground state and the M intermediate. This study indicated that the relative pK_a sensitively depends on the three-dimensional structure of the protein, especially on the structure of the hydrogen bonding network surrounding RSB. W402 and Thr89 are the main contributors for controlling the relative pK_a values. In particular, the side chain of Thr89 forms relatively strong hydrogen bonds with Asp85 in the M intermediate, consistent with the results from the recent FTIR studies. Thus, this residue is a key factor stabilizing the neutral state of the M intermediate. The results for the hypothetical proton pathway suggested that Thr89 is potentially important for the occurrence of unidirectional proton transfer, because the back proton transfer from the M intermediate may be kinetically inhibited in the presence of this residue.

Acknowledgment. The authors thank the Computer Center, Institute for Molecular Science, Okazaki, Japan, for the use of the supercomputer system. We also thank the Computer Center, Tokyo Institute of Technology, for the use of the SGI Origin 2000 system. This work was supported by Grant-in-Aid No. 12680653 from the Ministry of Education, Science, Sports, and Culture Japan.

References and Notes

(1) See for reviews: (a) Birge, R. R. *Annu. Rev. Phys. Chem.* **1990**, *41*, 683. (b) Lanyi, J. K. *Biochim. Biophys. Acta* **1993**, *1183*, 241. (c) Khorana, H. G. *Ann. N. Y. Acad. Sci.* **1986**, *471*, 272. (d) Mathies, R. A.; Lin, S. W.; Ames, J. B.; Pollard, W. T. *Annu. Rev. Biophys. Biophys. Chem.* **1991**, *20*, 491.

(2) Lozier, R.; Bogomlni, R. A.; Stoeckenius, W. *Biophys. J.* **1975**, *15*, 955.

(3) Lanyi, J. K. *J. Struct. Biol.* **1998**, *124*, 164.

(4) Haupts, U.; Tittor, J.; Oesterhelt, D. *Annu. Rev. Biophys. Biomol. Struct.* **1999**, *28*, 367.

(5) Spudich, J. K.; Lanyi, J. K. *Curr. Opin. Cell. Biol.* **1996**, *8*, 452.

(6) Subramaniam, S.; Lindahl, M.; Bullough, P.; Faruqi, A. R.; Tittor, J.; Oesterhelt, D.; Brown, L.; Lanyi, J.; Henderson, R. *J. Mol. Biol.* **1999**, *287*, 145.

(7) Kataoka, M.; Kamikubo, H.; Tokunaga, F.; Brown, L. S.; Yamazaki, Y.; Maeda, A.; Sheves, M.; Needleman, R.; Lanyi, J. K. *J. Mol. Biol.* **1994**, *243*, 621.

(8) Richter, H. T.; Brown, L. S.; Needleman, R.; Lanyi, J. K. *Biochemistry* **1996**, *35*, 4054.

(9) Maeda, A.; Sasaki, J.; Shichida, Y.; Yoshizawa, T. *Biochemistry* **1992**, *31*, 462.

(10) Hatanaka, M.; Kandori, H.; Maeda, A. *Biophys. J.* **1997**, *73*, 1001.

(11) Kandori, H.; Kinoshida, N.; Shichida, Y.; Maeda, A. *J. Phys. Chem. B* **1998**, *102*, 7899.

(12) Luecke, H.; Schobert, B.; Richter, H. T.; Cartailler, J. P.; Lanyi, J. K. *Science* **1999**, *286*, 255.

(13) Luecke, H.; Schobert, B.; Richter, H. T.; Cartailler, J. P.; Rosengarth, A.; Needleman, R.; Lanyi, J. K. *J. Mol. Biol.* **2000**, *300*, 1237.

(14) Sass, H. J.; Buldt, G.; Gessenich, R.; Hehn, D.; Neff, D.; Schlesinger, R.; Berendzen, J.; Ormos, P. *Nature* **2000**, *406*, 649.

(15) Baasov, T.; Sheves, M. *Biochemistry* **1986**, *25*, 5249.

(16) Rousso, I.; Friedman, N.; Sheves, M.; Ottolenghi, M. *Biochemistry* **1995**, *34*, 12059.

(17) Druckman, S.; Ottolenghi, M.; Pande, A.; Pande, J.; Callender, R. H. *Biochemistry* **1982**, *21*, 4953.

(18) Balashov, S. P.; Govindjee, R.; Ebrey, T. G. *Biophys. J.* **1991**, *60*, 475.

(19) Tajkhorshid, E.; Suhai, S. *J. Mol. Struct.: THEOCHEM* **2000**, *501*, 297.

(20) Murata, K.; Fujii, Y.; Enomoto, N.; Hata, M.; Hoshino, T.; Tsuda, M. *Biophys. J.* **2000**, *79*, 982.

(21) Tajkhorshid, E.; Paizs, B.; Suhai, S. *J. Phys. Chem. B* **1999**, *103*, 4518.

(22) Paizs, B.; Tajkhorshid, E.; Suhai, S. *J. Phys. Chem. B* **1999**, *103*, 5388.

(23) Hayashi, S.; Ohmine, I. *J. Phys. Chem. B* **2000**, *104*, 10678.

(24) Spassov, V. Z.; Luecke, H.; Gerwert, K.; Bashford, D. *J. Mol. Biol.* **2001**, *312*, 203.

(25) Ohno, K.; Kamiya, N.; Asakawa, N.; Inoue, Y.; Sakurai, M. *Chem. Phys. Lett.* **2001**, *341*, 387.

(26) Stewart, J. J. *Int. J. Quantum Chem.* **1996**, *58*, 133.

(27) Luecke, H.; Schobert, B.; Richter, H. T.; Cartailler, J. P.; Lanyi, J. K. *J. Mol. Biol.* **1999**, *291*, 899.

(28) Facciotti, M. T.; Rouhani, S.; Burkard, F. T.; Betancourt, F. M.; Downing, K. H.; Rose, R. B.; McDermott, G.; Glaeser, R. M. *Biophys. J.* **2001**, *81*, 3442.

(29) Takeda, K.; Matsui, Y.; Sato, H.; Hino, T.; Okumura, H.; Kanamori, E.; Yamane, T.; Kamiya, N.; Iizuka, T.; Adachi, S.; Kouyama, T. *4th International Conference on Biological Physics Abstracts*; Kyoto, 2001; p 50.

(30) Biosym/MSI Technologies, San Diego, CA, 1998.

(31) Sasaki, J.; Lanyi, J. K.; Needleman, R.; Yoshizawa, T.; Maeda, A. *Biochemistry* **1994**, *33*, 3178.

(32) Brown, L. S.; Sasaki, J.; Kandori, H.; Maeda, A.; Needleman, R.; Lanyi, J. K. *J. Biol. Chem.* **1995**, *270*, 27122.

(33) Dewar, M. J. S.; Zoebisch, E. G.; Stewart, J. J. *J. Am. Chem. Soc.* **1985**, *107*, 3902.

(34) Stewart, J. J. *MOPAC 2002*; Fujitu Ltd.: Tokyo, Japan, 1999.

(35) Frisch, M. J.; Trucks, G. W.; Schlegel, H. B.; Scuseria, G. E.; Robb, M. A.; Cheeseman, J. R.; Zakrzewski, V. G.; Montgomery, J. A., Jr.; Stratman, R. E.; Burant, J. C.; Dapprich, S.; Millam, J. M.; Daniels, A. D.; Kudin, K. N.; Strain, M. C.; Farkas, O.; Tomasi, J.; Barone, V.; Cossi, M.; Cammi, R.; Mennucci, B.; Pomelli, C.; Adamo, C.; Clifford, S.; Ochterski, J.; Petersson, G. A.; Ayala, P. Y.; Cui, Q.; Morokuma, K.; Malick, D. K.; Rabuck, A. D.; Raghavachari, K.; Foresman, J. B.; Cioslowski, J.; Ortiz, J.; Stefanov, B. B.; Liu, G.; Liashenko, A.; Piskorz, P.; Komaromi, I.; Gomperts, R.; Martin, R. L.; Fox, D. J.; Keith, T.; Al-Laham, M. A.; Peng, C. Y.; Nanayakkara, A.; Gonzalez, C.; Challacombe, M.; Gill, P. M. W.; Johnson, B. G.; Chen, W.; Wong, M. W.; Andres, J. L.; Head-Gordon, M.; Replogle, E. S.; Pople, J. A. *Gaussian 98*; Gaussian Inc.: Pittsburgh, PA, 1998.

(36) Jonas, R.; Koutalos, Y.; Ebrey, T. G. *Photochem. Photobiol.* **1990**, *52*, 1163.

(37) Brown, L. S.; Lanyi, J. K. *Proc. Natl. Acad. Sci. U.S.A.* **1996**, *93*, 1731.

(38) Braiman, M. S.; Dioumaev, A. K.; Lewis, J. R. *Biophys. J.* **1996**, *70*, 939.

(39) Scheiner, S.; Duan, X. *Biophys. J.* **1991**, *60*, 874.

(40) Lanyi, J. K.; Brigitte, S. *J. Mol. Biol.* **2002**, *321*, 727.

(41) Kandori, H.; Kinoshita, N.; Yamazaki, Y.; Maeda, A.; Shichida, Y.; Needleman, R.; Lanyi, J. K.; Bizounok, M.; Herzfeld, J.; Raap, J.; Lugtenburg, J. *Biochemistry* **1999**, *38*, 9676.

(42) Kandori, H.; Yamazaki, Y.; Shichida, Y.; Raap, J.; Lugtenburg, J.; Belenky, M.; Herzfeld, J. *Proc. Natl. Acad. Sci. U.S.A.* **2001**, *98*, 1571.

(43) Russell, T. S.; Coleman, M.; Rath, P.; Nilsson, A. Rothschild, K. *Biochemistry* **1997**, *36*, 7490.